JACS
JOURNAL OF THE AMERICAN CHEMICAL SOCIETY
pubs.acs.org/JACS
Communication

Room-Temperature Magnetic Bistability in a Salt of Organic Radical Ions

Anni I. Taponen, Awatef Ayadi, Manu K. Lahtinen, Itziar Oyarzabal, Sébastien Bonhommeau, Mathieu Rouzières, Corine Mathonière, Heikki M. Tuononen, Rodolphe Clérac,* and Aaron Mailman*

Cite This: https://doi.org/10.1021/jacs.1c07468
Read Online
ACCESS | Metrics & More | Article Recommendations | Supporting Information

ABSTRACT: Cocrystallization of 7,7′,8,8′-tetracyanoquinodimethane radical anion ($TCNQ^{-\bullet}$) and 3-methylpyridinium-1,2,3,5-dithiadiazolyl radical cation (3-MepyDTDA$^{+\bullet}$) afforded isostructural acetonitrile (MeCN) or propionitrile (EtCN) solvates containing cofacial π dimers of homologous components. Loss of lattice solvent from the diamagnetic solvates above 366 K affords a high-temperature paramagnetic phase containing discrete $TCNQ^{-\bullet}$ and weakly bound π dimers of 3-MepyDTDA$^{+\bullet}$, as evidenced by X-ray diffraction methods and magnetic susceptibility measurements. Below 268 K, a first-order phase transition occurs, leading to a low-temperature diamagnetic phase with $TCNQ^{-\bullet}$ σ dimer and π dimers of 3-MepyDTDA$^{+\bullet}$. This study reveals the first example of cooperative interactions between two different organic radical ions leading to magnetic bistability, and these results are central to the future design of multicomponent functional molecular materials.

Stable organic radicals that exhibit a hysteretic response to an external stimulus (temperature, light, or pressure) display physical properties such as magnetic bistability that are promising for use in nanotechnology devices.[1−6] Neutral organic π radicals have been extensively studied because their electron-exchange interactions can lead to dynamic structures weakly coupled; in which interconversion between radicals ($S = {}^1/_2$) and π or σ dimers ($S = 0$) is possible.[7−20] These cooperative solid-state interactions between different centers allow variation of the crystalline lattice such that hysteretic first-order phase transitions can arise. While this parallels the well-known spin-crossover (SCO) phenomena of transition metal ion complexes,[6] radical-based magnetically bistable systems are comparatively rare. The neutral heterocyclic thiazyl π radicals are among the most successful class of radicals in this regard,[7,9,11,13−18] with only a few examples of nitroxides[8,21−24], triazinyl[25] and spirophenalenyl[26] derivatives known to be bistable. In these examples, magnetic switching typically occurs by breaking/forming antiferromagnetically coupled π dimers, although examples of weakly bonded σ dimers have also been reported.[9,11]

The recently described intramolecular electron exchange in discrete neutral[21,27] and ionic diradicals[10] provides insights into how chemical and electronic structure affects the bistable behavior and the importance of cooperative interactions in the solid state. In this context, we chose to explore the cocrystallization of two different radical ions in a salt to couple the structural and electron-exchange interactions in the solid state.[28] The recently reported 4-(*N*-methylpyridinium-3-yl)-1,2,3,5-dithiadiazolyl radical cation (3-MepyDTDA$^{+\bullet}$)[29] was chosen as the positive radical ion. These DTDA radicals readily form π dimers in the solid state (Chart 1) despite their cationic pyridinium substituent (−R) and are ideal candidates for crystal engineering through intermolecular $S^{\delta+}\cdots N^{\delta-}$ interactions. The quintessential electron acceptor 7,7′,8,8′-tetracyanoquinodimethane (TCNQ) was chosen as a partner for MepyDTDA$^{+\bullet}$ because it forms stable π radical anions ($TCNQ^{-\bullet}$) and its cyanido substituents can act as structure-directing groups. Relatedly, the cation can influence the geometry of $TCNQ^{-\bullet}$ in the solid state, such that discrete π

Chart 1. Common Modes of Dimerization in Substituted 1,2,3,5-Dithiadiazolyl (DTDA) Radicals and 7,7′,8,8′-Tetracyanoquinodimethane (TCNQ) Radical Anion

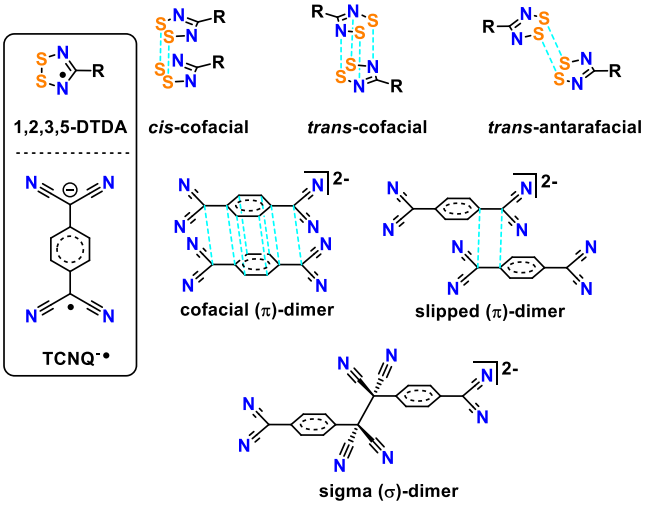

Received: July 18, 2021

radical anions and/or its π or σ dimers can be observed in the solid state (Chart 1).[30−35] In this work, we demonstrate a surprising twofold single-crystal-to-single-crystal transformation[36−39] involving both the π and σ dimers of $TCNQ^{-\bullet}$ and discrete $TCNQ^{-\bullet}$ radical anion geometries, leading to thermal bistability at room temperature.

A double-displacement reaction between the 18-crown-6 ether (18c6) potassium complex[40] of $TCNQ^{-\bullet}$ and [3-MepyDTDA][OTf] in acetonitrile (MeCN) or propionitrile (EtCN) afforded the 1:1 radical ion salt [3-MepyDTDA][TCNQ] (**1**) as a MeCN or EtCN solvate, respectively (Scheme 1). The two solvates are isostructural, crystallizing in

Scheme 1. Double-Displacement Reaction between [K(18c6)][TCNQ] and [3-MepyDTDA][OTf] to Afford 1·RCN and [K(18c6)][OTf]

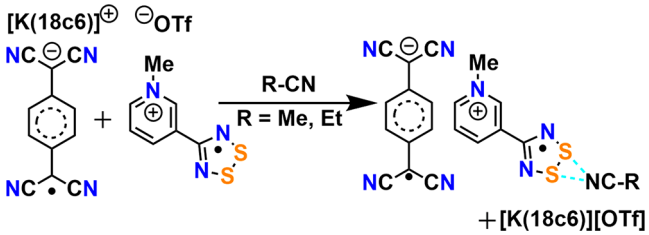

a triclinic unit cell ($P\bar{1}$) containing *trans*-cofacial dimers of 3-MepyDTDA$^{+\bullet}$ and cofacial dimers of $TCNQ^{-\bullet}$ (Chart 1). Each 3-MepyDTDA$^{+\bullet}$ obliquely interacts with one solvent molecule via supramolecular S···N′ contacts (Figure 1a) that are shorter than the sum of the van der Waals radii (ca. 3.26 Å).[41,42] The solvates form alternating $A^+A^+B^-B^-$ π stacks, with hydrogen bonding between the out-of-register neighboring stacks (Figure S13).

Thermogravimetric analysis (TGA) of crystalline samples indicated the onset of desolvation of **1**·EtCN at 365 K, while the loss of lattice solvent from **1**·MeCN occurred with a noticeably higher onset temperature of 396 K. The solvent stoichiometry was verified by the percentage weight loss found from the TGA curve, and the results are consistent with the crystal structures. Both **1**·MeCN and **1**·EtCN displayed high thermal stability after the desolvation alteration, with the onset of decomposition occurring above 480 K (Figures S4−S7 and Table S1).

Variable-temperature magnetic measurements were performed on microcrystalline samples of both **1**·MeCN and **1**·EtCN to determine the effects of the thermal processes on the physical properties. The magnetic susceptibilities of **1**·MeCN and **1**·EtCN were studied over a temperature range of 1.85−400 K in both cooling and heating modes (Figure S9). Both solvates are diamagnetic solids upon cooling from room temperature. Upon heating, however, they displayed a sudden surge in the χT product at temperatures approaching the desolvation onset temperatures recorded by TGA (Figure S4). In the case of **1**·EtCN, the onset of this surge occurs at 350 K, and the χT product rises to 0.38 cm^3 K mol^{-1} at 400 K, which is close to the value of 0.375 cm^3 K mol^{-1} predicted for an $S = {}^1/_2$ Curie paramagnet (g = 2.00). Under identical conditions, the desolvation of **1**·MeCN was less effective, as the χT product reached a value of only 0.24 cm^3 K mol^{-1} at 400 K, the limit of our experiment. Remarkably, the newly formed paramagnetic and desolvated phase did not follow the same track upon cooling, and an abrupt decrease in χT was recorded

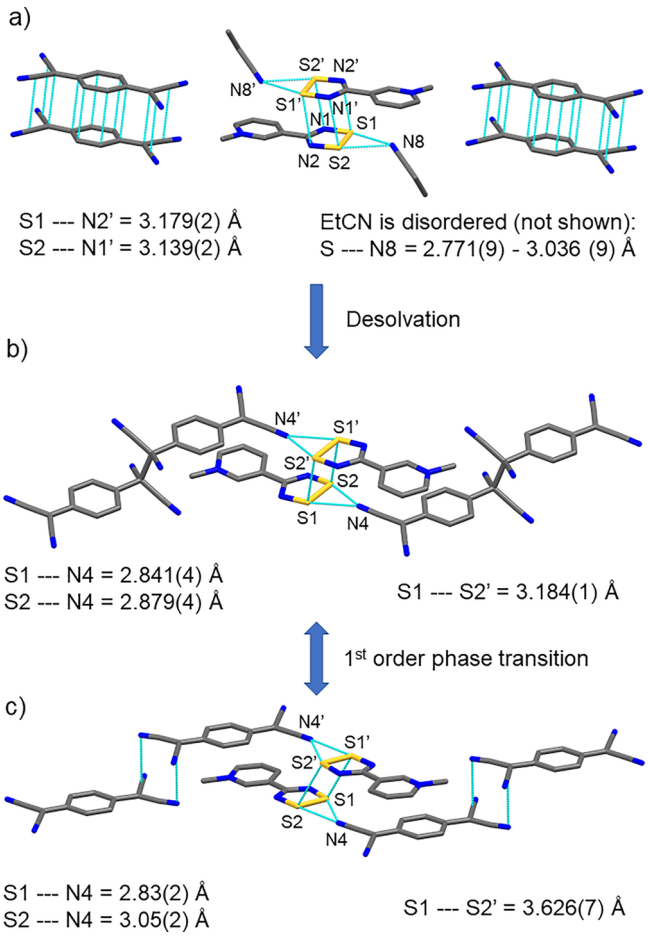

Figure 1. Representative view of the intermolecular interactions in (a) the solvate **1**·EtCN ($P\bar{1}$) at 120 K, (b) the LT phase of **1** ($P2_1/n$) at 120 K, and (c) the HT phase of **1** ($P2_1/n$) at 340 K. Sulfur is shown in yellow, nitrogen in blue, and carbon in gray.

below 290 K. Subsequent heating and cooling cycles indicated a hysteretic response of the magnetic susceptibility near room temperature (263−294 K), consistent with a first-order phase transition for both desolvated **1**·EtCN and **1**·MeCN materials (Figures S10 and S11).

Motivated by the TGA and magnetic susceptibility results, we attempted the desolvation of a crystalline sample of **1**·EtCN. Satisfyingly, after careful heating in vacuo (353−395 K, 10^{-2} bar) over 2 days, crystals suitable for single-crystal X-ray diffraction studies were obtained. Interestingly, the loss of lattice solvent afforded crystals belonging to a higher-symmetry monoclinic ($P2_1/n$) unit cell at 120 K. This low-temperature (LT) phase contains *trans*-antarafacial dimers of 3-MepyDTDA$^{+\bullet}$ with short intermolecular S−S′ contacts (3.184(1) Å), while the TCNQ radicals are now σ-dimerized via a long C−C bond (1.656(8) Å), in contrast to the π dimers found in the solvates (Figure 1b). The newly formed tetrahedral (sp^3) carbon of the σ dimer forces the dicyanomethyl group to project toward the *ab* plane, and this geometry provides a nook where the methyl substituent of the pyridinium ring is nested. The resulting layered structure forms zigzag chains that adopt a chevron motif through short intermolecular CN−S contacts (Figures 1b and S14−S16). The packing optimizes the electrostatic interactions of the terminal dicyanomethanide portion of the σ dimer and the pyridinium ring, affording an array of secondary hydrogen bonding.

https://doi.org/10.1021/jacs.1c07468
J. Am. Chem. Soc. XXXX, XXX, XXX−XXX

The LT phase remains unchanged as it is warmed to 260 K (just below the transition temperature observed by magnetic measurements in Figures S10 and S11), with the σ dimer C−C bond length (1.662(5) Å) not significantly changed. However, a modest change in the β angle from 97.1° to 96.4° and a slight increase in the intermolecular S···S′ interactions occur (Figure 1b and Table S3). At 340 K (above the transition temperature), the monoclinic $P2_1/n$ unit cell is conserved, with a marked change in the β angle from 96.4° to 91.8°. The crystal structure obtained from the high-temperature (HT) data provided clear evidence for discrete TCNQ radicals and significant elongation of the intradimer S−S′ contacts between 3-MepyDTDA$^{+\bullet}$ radicals to 3.626(7) Å (Figure 1c). This value is near the sum of the van der Waals radii of two sulfur atoms (ca. 3.60 Å).[41,42] The layered zigzag chains and the chevron packing of the LT phase are largely maintained in the HT phase along with short intermolecular CN···S contacts between neighboring TCNQ$^{-\bullet}$ and 3-MepyDTDA$^{+\bullet}$ radicals within the same zigzag chain (Figures 1c and S17−S20). Because of the cleavage of the C−C-bonded σ dimer, the two open-shell ($S = {}^1/_2$) TCNQ$^{-\bullet}$ radical anions slip over an inversion center with an interplanar separation of 3.331 Å.

Powder X-ray diffraction (PXRD) data collected for **1**·MeCN (Figure S21) and **1**·EtCN (Figure S22) at room temperature demonstrated that the bulk phases of both solvates are structurally like the corresponding single-crystal structures. Heating of these samples at various intervals up to 417 K led to a shift of diffraction peaks in the powder pattern along with marked changes in the intensities (Figures S23 and S24). This leads to an HT phase of **1** that contains residual traces of **1**·EtCN. However, subsequent cooling clearly indicated a phase transition to the LT phase below 250 K. The HT phase was recovered upon warming to room temperature. Pawley analyses of the collected patterns were consistent with the unit cell parameters obtained from the single-crystal structures (Figure 2 and Tables S4 and S5).

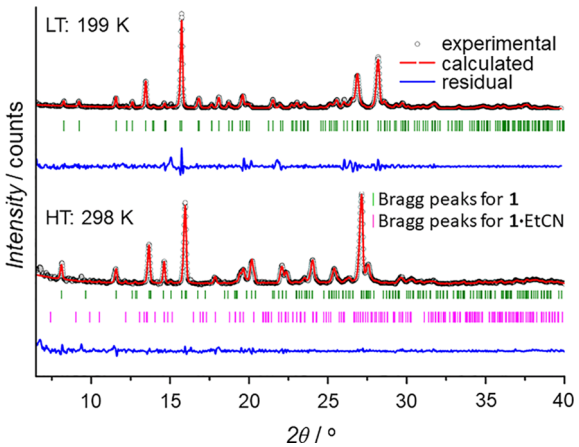

Figure 2. PXRD patterns of the LT phase (top) and HT phase (bottom) obtained by in situ desolvation of **1**·EtCN.

Similar results were obtained for **1**·MeCN (Figure S25), but the TGA results indicated that MeCN is more difficult to remove from the crystal lattice. A solvent-free HT phase of **1** could be most easily obtained by careful heating of crystalline **1**·EtCN in vacuo to achieve desolvation, as evidenced by TGA and Fourier transform infrared (FTIR) spectroscopy (the absence of ν(C≡N) at 2248 cm^{-1} assigned to EtCN; Figure S3) and verified by satisfactory elemental analyses consistent with solvent-free **1**.

The magnetothermal behavior of **1** (Figures 3 and S12) is consistent with the measurements performed on the solvates.

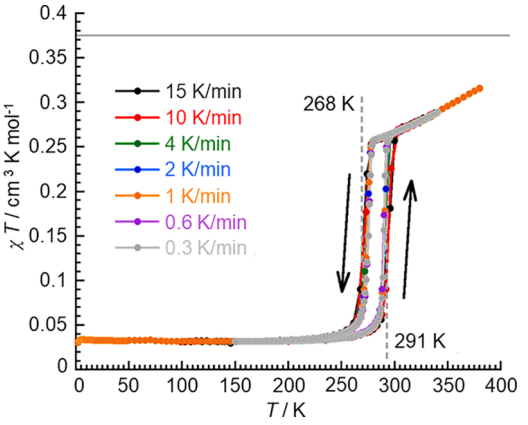

Figure 3. Temperature dependence of the χT product between 1.85 and 380 K measured for **1** at 1 T at different heating−cooling rates. The gray line indicates the expected χT value for an $S = {}^1/_2$ and $g = 2$ Curie paramagnet.

The χT product rises continuously above the transition temperature $T_{1/2}\uparrow$ = 291 K (where $T_{1/2}$ is the temperature at which the LT and HT phases coexist as a 1:1 mixture and ↑ and ↓ arrows indicate that $T_{1/2}$ was measured in heating and cooling mode, respectively) but does not reach the value of 0.375 cm^3 K mol^{-1} expected for an $S = {}^1/_2$ Curie paramagnet (g = 2.00). This suggests that in the HT phase, intramolecular antiferromagnetic (AFM) interactions are present between the TCNQ$^{-\bullet}$ radical anions but the π dimers of 3-MepyDTDA$^{+\bullet}$ remain diamagnetic. Below $T_{1/2}\downarrow$ = 268 K, the χT product decreases and is essentially temperature-independent, consistent with a diamagnetic LT phase. The hysteresis loop between 268 and 291 K appears to be unaltered when cycled between high (15 K min^{-1}) and low (0.3 K min^{-1}) heating−cooling rates, indicating that the dynamics of this first-order phase transition is slower than our experimental time scales.

Differential scanning calorimetry (DSC) data collected on **1** demonstrated a reversible thermal solid−solid transition associated with the structural interconversion between the HT and LT phases of **1** (Figure 4). Nearly identical enthalpies of change (ca. 7 kJ mol^{-1}) were recorded during the heating and cooling phases, highlighting the reproducibility of the thermal process.

Interestingly, in related salts containing the σ dimer of TCNQ$^{-\bullet}$, thermal cleavage to form paramagnetic species has been evidenced only by solid-state electron paramagnetic resonance (EPR) measurements. However, the estimated energies reported for C−C σ-bond cleavage are much greater (24 kJ mol^{-1})[43−45] and occur above 400 K without evidence for a first-order phase transition.

A spectroscopic signature for the phase transition from the HT phase to the LT phase of **1** was measured by Raman and FTIR spectroscopies (Figures 5 and S26−S32). The room-temperature spectra are dominated by stretching modes attributed to TCNQ$^{-\bullet}$. Below 270 K there is a clear difference between the spectra, as multiple ν(C≡N) stretching modes appear in line with σ dimerization.

https://doi.org/10.1021/jacs.1c07468
J. Am. Chem. Soc. XXXX, XXX, XXX−XXX

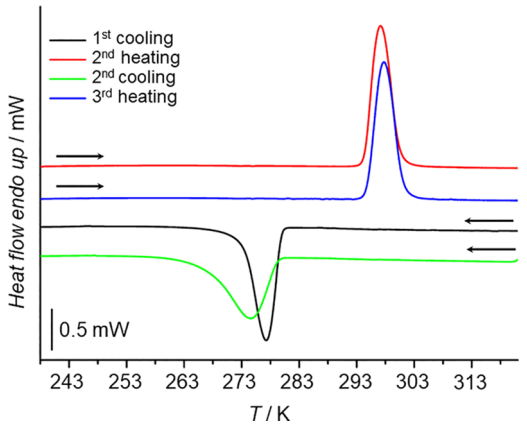

Figure 4. DSC curves of different heating−cooling (10 K min^{-1}) scans for **1**. Scans are shifted on the *y* axis for clarity, and the first heating (not shown) was from 298 to 423 K to verify complete desolvation before the first cooling cycle (see Figure S8).

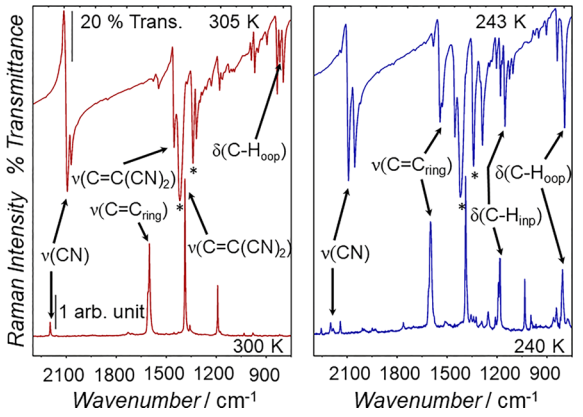

Figure 5. (top) FTIR and (bottom) Raman spectra of the HT phase (red) and LT phase (blue) of **1** with tentative assignments of stretching (ν) and bending (δ) modes (inp = in-plane) of $TCNQ^{-\bullet}$ and its σ dimer. The LT phase displays bending modes, $\delta(C{-}H_{inp})$, and a strong absorption at 798 cm^{-1} (cf. 806 cm^{-1})[47] assigned to the $\delta(C{-}H_{oop})$ bending mode (Raman-active only for the σ dimer) attributed to the σ dimer. Asterisks denote Nujol mull peaks.

Complementary information obtained by FTIR spectroscopy indicated a $\delta(C{-}H)$ bending mode at 822 cm^{-1}, in agreement with the presence of $TCNQ^{-\bullet}$.[46−48] Lastly, the Raman and IR spectra of the LT phase of **1** are consistent with spectra measured for the σ dimer of $TCNQ^{-\bullet}$ found in the ethylphenazenium ($EtPhen^{+}$) salt,[32,43] validating the spectral changes for the phase transition in **1**.

To summarize, we have established that the crystalline solvates **1**·RCN (R = Me, Et) containing $TCNQ^{-\bullet}$ and 3-MepyDTDA$^{+\bullet}$ π dimers tolerate loss of lattice solvent, leading to an HT phase of **1** that undergoes a reversible first-order phase transition associated with the structural interconversion between discrete $TCNQ^{-\bullet}$ radical anions ($S = {}^{1}/_{2}$) and their C−C-bonded σ dimers ($S = 0$). The single-crystal X-ray data illustrate the cooperative role of the structurally flexible π dimer of 3-MepyDTDA$^{+\bullet}$ and the intermolecular $S^{\delta+}{-}N^{\delta-}$ interactions that bookend the discrete $TCNQ^{-\bullet}$ radical anions. While spin pairing in planar organic radicals typically occurs through overlap of their π orbitals, salt **1** is a relatively rare example of a σ dimer exhibiting magnetic bistability behavior. Furthermore, **1** is an unprecedented example of a two-component magnetically bistable system composed solely of molecular organic radicals and provides impetus for further investigations on related σ dimer systems containing TCNQ and their potential for functional organic materials.

■ ASSOCIATED CONTENT

Supporting Information

The Supporting Information is available free of charge at https://pubs.acs.org/doi/10.1021/jacs.1c07468.

Full description of experimental details, including additional IR, Raman, TGA, DSC, magnetic susceptibility, PXRD, and X-ray diffraction data and illustrations (PDF)

Accession Codes

CCDC 2097021−2097025 contain the supplementary crystallographic data for this paper. These data can be obtained free of charge via www.ccdc.cam.ac.uk/data_request/cif, or by emailing data_request@ccdc.cam.ac.uk, or by contacting The Cambridge Crystallographic Data Centre, 12 Union Road, Cambridge CB2 1EZ, U.K.; fax: +44 1223 336033.

■ AUTHOR INFORMATION

Corresponding Authors

Aaron Mailman − *NanoScience Centre, Department of Chemistry, University of Jyväskylä, FI-40014 Jyväskylä, Finland;* orcid.org/0000-0003-2067-8479; Email: aaron.m.mailman@jyu.fi

Rodolphe Clérac − *Univ. Bordeaux, CNRS, Centre de Recherche Paul Pascal, UMR5031, F-33600 Pessac, France;* orcid.org/0000-0001-5429-7418; Email: clerac@crpp-bordeaux.cnrs.fr

Authors

Anni I. Taponen − *NanoScience Centre, Department of Chemistry, University of Jyväskylä, FI-40014 Jyväskylä, Finland*

Awatef Ayadi − *NanoScience Centre, Department of Chemistry, University of Jyväskylä, FI-40014 Jyväskylä, Finland*

Manu K. Lahtinen − *NanoScience Centre, Department of Chemistry, University of Jyväskylä, FI-40014 Jyväskylä, Finland;* orcid.org/0000-0001-5561-3259

Itziar Oyarzabal − *Univ. Bordeaux, CNRS, Centre de Recherche Paul Pascal, UMR5031, F-33600 Pessac, France; BCMaterials, Basque Center for Materials, Applications and Nanostructures, ES-48940 Leioa, Spain; IKERBASQUE, Basque Foundation for Science, ES-48009 Bilbao, Spain;* orcid.org/0000-0001-9149-2511

Sébastien Bonhommeau − *Univ. Bordeaux, CNRS, Bordeaux INP, ISM, UMR5255, F-33400 Talence, France;* orcid.org/0000-0002-9213-7201

Mathieu Rouzières − *Univ. Bordeaux, CNRS, Centre de Recherche Paul Pascal, UMR5031, F-33600 Pessac, France*

Corine Mathonière − *Univ. Bordeaux, CNRS, Centre de Recherche Paul Pascal, UMR5031, F-33600 Pessac, France*

Heikki M. Tuononen − *NanoScience Centre, Department of Chemistry, University of Jyväskylä, FI-40014 Jyväskylä, Finland;* orcid.org/0000-0002-4820-979X

Complete contact information is available at: https://pubs.acs.org/10.1021/jacs.1c07468

Notes

The authors declare no competing financial interest.

■ ACKNOWLEDGMENTS

The contributions of Noora Svahn to the preparation of starting materials and Elina Hautakangas for assistance with elemental analysis are gratefully acknowledged. A.M. and H.M.T. thank the Academy of Finland for funding (Projects 333565, 336456, and 289172). R.C., C.M., M.R., and I.O. received funding from the University of Bordeaux, the Region Nouvelle Aquitaine, Quantum Matter Bordeaux, and the Centre National de la Recherche Scientifique (CNRS). Raman measurements were performed at the SIV platform funded by the European Union (FEDER) and the Nouvelle Aquitaine Region.

■ REFERENCES

(1) Sato, O. Dynamic Molecular Crystals with Switchable Physical Properties. *Nat. Chem.* **2016**, *8* (7), 644−656.
(2) Ratera, I.; Veciana, J. Playing with Organic Radicals as Building Blocks for Functional Molecular Materials. *Chem. Soc. Rev.* **2012**, *41* (1), 303−349.
(3) Hicks, R. G. A New Spin on Bistability. *Nat. Chem.* **2011**, *3* (3), 189−191.
(4) Hicks, R. *Stable Radicals: Fundamentals and Applied Aspects of Odd-Electron Compounds*; Wiley, 2011.
(5) Rawson, J. M.; Alberola, A.; Whalley, A. Thiazyl Radicals: Old Materials for New Molecular Devices. *J. Mater. Chem.* **2006**, *16* (26), 2560−2575.
(6) Rawson, J. M.; Hayward, J. J. Reversible Spin Pairing in Crystalline Organic Radicals. In *Spin-Crossover Materials*; Wiley, 2013; pp 225−237.
(7) Richardson, J. G.; Mizuno, A.; Shuku, Y.; Awaga, K.; Robertson, N.; Morrison, C. A.; Warren, M. R.; Allan, D. R.; Moggach, S. A. Evaluating the High-Pressure Structural Response and Crystal Lattice Interactions of the Magnetically-Bistable Organic Radical TTTA. *CrystEngComm* **2021**, *23*, 4444−4450.
(8) Dragulescu-Andrasi, A.; Filatov, A. S.; Oakley, R. T.; Li, X.; Lekin, K.; Huq, A.; Pak, C.; Greer, S. M.; McKay, J.; Jo, M.; Lengyel, J.; Hung, I.; Maradzike, E.; DePrince, A. E.; Stoian, S. A.; Hill, S.; Hu, Y.-Y.; Shatruk, M. Radical Dimerization in a Plastic Organic Crystal Leads to Structural and Magnetic Bistability with Wide Thermal Hysteresis. *J. Am. Chem. Soc.* **2019**, *141* (45), 17989−17994.
(9) Bates, D.; Robertson, C. M.; Leitch, A. A.; Dube, P. A.; Oakley, R. T. Magnetic Bistability in Naphtho-1,3,2-Dithiazolyl: Solid State Interconversion of a Thiazyl π-Radical and Its N−N σ-Bonded Dimer. *J. Am. Chem. Soc.* **2018**, *140* (11), 3846−3849.
(10) Li, T.; Tan, G.; Shao, D.; Li, J.; Zhang, Z.; Song, Y.; Sui, Y.; Chen, S.; Fang, Y.; Wang, X. Magnetic Bistability in a Discrete Organic Radical. *J. Am. Chem. Soc.* **2016**, *138* (32), 10092−10095.
(11) Lekin, K.; Winter, S. M.; Downie, L. E.; Bao, X.; Tse, J. S.; Desgreniers, S.; Secco, R. A.; Dube, P. A.; Oakley, R. T. Hysteretic Spin Crossover between a Bisdithiazolyl Radical and Its Hypervalent σ-Dimer. *J. Am. Chem. Soc.* **2010**, *132* (45), 16212−16224.
(12) Clarke, C. S.; Jornet-Somoza, J.; Mota, F.; Novoa, J. J.; Deumal, M. Origin of the Magnetic Bistability in Molecule-Based Magnets: A First-Principles Bottom-Up Study of the TTTA Crystal. *J. Am. Chem. Soc.* **2010**, *132* (50), 17817−17830.
(13) Brusso, J. L.; Clements, O. P.; Haddon, R. C.; Itkis, M. E.; Leitch, A. A.; Oakley, R. T.; Reed, R. W.; Richardson, J. F. Bistabilities in 1,3,2-Dithiazolyl Radicals. *J. Am. Chem. Soc.* **2004**, *126* (26), 8256−8265.
(14) Brusso, J. L.; Clements, O. P.; Haddon, R. C.; Itkis, M. E.; Leitch, A. A.; Oakley, R. T.; Reed, R. W.; Richardson, J. F. Bistability and the Phase Transition in 1,3,2-Dithiazolo[4,5-*b*]pyrazin-2-yl. *J. Am. Chem. Soc.* **2004**, *126* (45), 14692−14693.
(15) Fujita, W.; Awaga, K. Room-Temperature Magnetic Bistability in Organic Radical Crystals. *Science* **1999**, *286* (5438), 261−262.
(16) Fujita, W.; Awaga, K.; Matsuzaki, H.; Okamoto, H. Room-Temperature Magnetic Bistability in Organic Radical Crystals: Paramagnetic-Diamagnetic Phase Transition in 1,3,5-Trithia-2,4,6-Triazapentalenyl. *Phys. Rev. B: Condens. Matter Mater. Phys.* **2002**, *65* (6), 064434.
(17) McManus, G. D.; Rawson, J. M.; Feeder, N.; van Duijn, J.; McInnes, E. J. L.; Novoa, J. J.; Burriel, R.; Palacio, F.; Oliete, P. Synthesis, Crystal Structures, Electronic Structure and Magnetic Behaviour of the Trithiatriazapentalenyl Radical, $C_2S_3N_3$. *J. Mater. Chem.* **2001**, *11* (8), 1992−2003.
(18) Du, H.; Haddon, R. C.; Krossing, I.; Passmore, J.; Rawson, J. M.; Schriver, M. J. Thermal Hysteresis in Dithiadiazolyl and Dithiazolyl Radicals Induced by Supercooling of Paramagnetic Liquids Close to Room Temperature: A Study of $F_3CCNSSN$ and an Interpretation of the Behaviour of $F_3CCSNSCCF_3$. *Chem. Commun.* **2002**, No. 17, 1836−1837.
(19) Alberola, A.; Eisler, D. J.; Harvey, L.; Rawson, J. M. Molecular Tailoring of Spin-Transition Materials: Preparation, Crystal Structure and Magnetism of Trifluoromethyl-Pyridyl-1,3,2-Dithiazolyl. *CrystEngComm* **2011**, *13* (6), 1794−1796.
(20) Matsuzaki, H.; Fujita, W.; Awaga, K.; Okamoto, H. Photo-induced Phase Transition in an Organic Radical Crystal with Room-Temperature Optical and Magnetic Bistability. *Phys. Rev. Lett.* **2003**, *91* (1), 017403.
(21) Shultz, D. A.; Fico, R. M., Jr.; Boyle, P. D.; Kampf, J. W. Observation of a Hysteretic Phase Transition in a Crystalline Dinitroxide Biradical That Leads to Magnetic Bistability. *J. Am. Chem. Soc.* **2001**, *123* (42), 10403−10404.
(22) Matsumoto, S.; Higashiyama, T.; Akutsu, H.; Nakatsuji, S. A Functional Nitroxide Radical Displaying Unique Thermochromism and Magnetic Phase Transition. *Angew. Chem., Int. Ed.* **2011**, *50* (46), 10879−10883.
(23) Nishimaki, H.; Ishida, T. Organic Two-Step Spin-Transition-Like Behavior in a Linear S = 1 Array: 3′-Methylbiphenyl-3,5-diyl Bis(*tert*-butylnitroxide) and Related Compounds. *J. Am. Chem. Soc.* **2010**, *132* (28), 9598−9599.
(24) Nishimaki, H.; Mashiyama, S.; Yasui, M.; Nogami, T.; Ishida, T. Bistable Polymorphs Showing Diamagnetic and Paramagnetic States of an Organic Crystalline Biradical Biphenyl-3,5-diyl Bis(*tert*-butylnitroxide). *Chem. Mater.* **2006**, *18* (16), 3602−3604.
(25) Constantinides, C. P.; Berezin, A. A.; Zissimou, G. A.; Manoli, M.; Leitus, G. M.; Bendikov, M.; Probert, M. R.; Rawson, J. M.; Koutentis, P. A. A Magnetostructural Investigation of an Abrupt Spin Transition for 1-Phenyl-3-trifluoromethyl-1,4-dihydrobenzo[*e*]-[1,2,4]triazin-4-yl. *J. Am. Chem. Soc.* **2014**, *136* (34), 11906−11909.
(26) Itkis, M. E.; Chi, X.; Cordes, A. W.; Haddon, R. C. Magneto-Opto-Electronic Bistability in a Phenalenyl-Based Neutral Radical. *Science* **2002**, *296* (5572), 1443.
(27) Peterson, J. P.; Zhang, R.; Winter, A. H. Effect of Structure on the Spin Switching and Magnetic Bistability of Solid-State Aryl Dicyanomethyl Monoradicals and Diradicals. *ACS Omega* **2019**, *4* (8), 13538−13542.
(28) Nascimento, M. A.; Heyer, E.; Clarke, J. J.; Cowley, H. J.; Alberola, A.; Stephaniuk, N.; Rawson, J. M. On the Design of Radical-Radical Cocrystals. *Angew. Chem., Int. Ed.* **2019**, *58* (5), 1371−1375.
(29) Taponen, A. I.; Wong, J. W. L.; Lekin, K.; Assoud, A.; Robertson, C. M.; Lahtinen, M.; Clérac, R.; Tuononen, H. M.; Mailman, A.; Oakley, R. T. Non-Innocent Base Properties of 3- and 4-Pyridyl-Dithia- and Diselenadiazolyl Radicals: The Effect of N-Methylation. *Inorg. Chem.* **2018**, *57* (21), 13901−13911.
(30) Garcia-Yoldi, I.; Miller, J. S.; Novoa, J. J. Theoretical Study of the Electronic Structure of $[TCNQ]_2^{2-}$ (TCNQ = 7,7,8,8-Tetracyano-*p*-Quinodimethane) Dimers and Their Intradimer, Long, Multicenter Bond in Solution and the Solid State. *J. Phys. Chem. A* **2009**, *113* (25), 7124−7132.

https://doi.org/10.1021/jacs.1c07468
J. Am. Chem. Soc. XXXX, XXX, XXX−XXX

(31) Grossel, M. C.; Evans, F. A.; Hriljac, J. A.; Prout, K.; Weston, S. C. Triplet Excitons in Isolated $TCNQ^{\bullet -}$ Dimers (TCNQ = Tetracyanoquinodimethane). *J. Chem. Soc., Chem. Commun.* **1990**, 1494−1495.
(32) Melby, L. R. Substituted Quinodimethans: VIII. Salts Derived from the 7,7,8,8-Tetracyanoquinodimethan Anion-Radical and Benzologues of Quaternary Pyrazinium Cations. *Can. J. Chem.* **1965**, *43* (5), 1448−1453.
(33) Ballester, L.; Gutiérrez, A.; Perpiñán, M. F.; Azcondo, M. T.; Sánchez, A. E. Interactions of TCNQ in Iron and Nickel Coordination Compounds. *Synth. Met.* **2001**, *120* (1), 965−966.
(34) Dong, V.; Endres, H.; Keller, H. J.; Moroni, W.; Nöthe, D. Dimerization of 7,7,8,8-Tetracyanoquinodimethane (TCNQ) Radical Anions It via σ-Bond Formation: Crystal Structure and EPR Properties of Bis(dipyridyl)platinum(II)-TCNQ, $[Pt(2,2'\text{-Dipy})_2^{2+}(TCNQ)_2^{2-}]$. *Acta Crystallogr., Sect. B: Struct. Crystallogr. Cryst. Chem.* **1977**, *33* (8), 2428−2431.
(35) Radhakrishnan, T. P.; Van Engen, D.; Soos, Z. G. Diamagnetic to Paramagnetic Transition in Trisdimethylaminocyclopropenium Tetracyanoquinodimethanide (TDAC-TCNQ). *Mol. Cryst. Liq. Cryst.* **1987**, *150* (1), 473−492.
(36) Yelgaonkar, S. P.; Campillo-Alvarado, G.; MacGillivray, L. R. Phototriggered Guest Release from a Nonporous Organic Crystal: Remarkable Single-Crystal-to-Single-Crystal Transformation of a Binary Cocrystal Solvate to a Ternary Cocrystal. *J. Am. Chem. Soc.* **2020**, *142* (49), 20772−20777.
(37) Chaudhary, A.; Mohammad, A.; Mobin, S. M. Recent Advances in Single-Crystal-to-Single-Crystal Transformation at the Discrete Molecular Level. *Cryst. Growth Des.* **2017**, *17* (5), 2893−2910.
(38) Liu, J.-L.; Wu, J.-Y.; Huang, G.-Z.; Chen, Y.-C.; Jia, J.-H.; Ungur, L.; Chibotaru, L. F.; Chen, X.-M.; Tong, M.-L. Desolvation-Driven 100-Fold Slow-down of Tunneling Relaxation Rate in Co(II)-Dy(III) Single-Molecule Magnets through a Single-Crystal-to-Single-Crystal Process. *Sci. Rep.* **2015**, *5* (1), 16621.
(39) Hao, Z.-M.; Zhang, X.-M. Solvent Induced Molecular Magnetic Changes Observed in Single-Crystal-to-Single-Crystal Transformation. *Dalton Trans* **2011**, *40* (10), 2092−2098.
(40) Schelter, E. J.; Morris, D. E.; Scott, B. L.; Thompson, J. D.; Kiplinger, J. L. Toward Actinide Molecular Magnetic Materials: Coordination Polymers of U(IV) and the Organic Acceptors TCNQ and TCNE. *Inorg. Chem.* **2007**, *46* (14), 5528−5536.
(41) Bondi, A. Van Der Waals Volumes and Radii. *J. Phys. Chem.* **1964**, *68*, 441−451.
(42) Politzer, P.; Murray, J. S. The Use and Misuse of van Der Waals Radii. *Struct. Chem.* **2021**, *32* (2), 623−629.
(43) Harms, R. H.; Keller, H. J.; Nöthe, D.; Werner, M.; Gundel, D.; Sixl, H.; Soos, Z. G.; Metzger, R. M. Triplet Spin Excitons in a Sigma-Bonded TCNQ Dimer Salt: *N*-Ethylphenazinium TCNQ, $(NEP^{+})_2(TCNQ^{-}-TCNQ^{-})$. *Mol. Cryst. Liq. Cryst.* **1981**, *65* (3−4), 179−196.
(44) Hatfield, W. E.; Hoffmann, S. K.; Corvan, P. J.; Singh, P.; Sethulekshmi, C. N.; Metzger, R. M. Excited Triplet State EPR of Sigma-bonded TCNQ Dimers in $[Cu(DMP)_2]_2[TCNQ]_2$. *J. Phys. Colloq.* **1983**, *44* (C3), C3-1377−C3-1380.
(45) Hoffmann, S. K.; Corvan, P. J.; Singh, P.; Sethulekshmi, C. N.; Metzger, R. M.; Hatfield, W. E. Crystal Structure and Excited Triplet-State Electron Paramagnetic Resonance of the. SIGMA.-Bonded TCNQ Dimer in Bis(2,9-Dimethyl-1,10-Phenanthroline)Copper(I) Tetracyanoquinodimethane Dimer $[Cu(DMP)_2]_2[TCNQ]_2$. *J. Am. Chem. Soc.* **1983**, *105* (14), 4608−4617.
(46) Zhao, H.; Heintz, R. A.; Ouyang, X.; Dunbar, K. R.; Campana, C. F.; Rogers, R. D. Spectroscopic, Thermal, and Magnetic Properties of Metal/TCNQ Network Polymers with Extensive Supramolecular Interactions between Layers. *Chem. Mater.* **1999**, *11* (3), 736−746.
(47) Zhao, H.; Heintz, R. A.; Dunbar, K. R.; Rogers, R. D. Unprecedented Two-Dimensional Polymers of Mn(II) with $TCNQ^{-\bullet}$ (TCNQ = 7,7,8,8-Tetracyanoquinodimethane). *J. Am. Chem. Soc.* **1996**, *118* (50), 12844−12845.
(48) Pukacki, W.; Pawlak, M.; Graja, A.; Lequan, M.; Lequan, R. M. Electronic and Spectral Properties of Organometallic Tetracyano-*p*-Quinodimethane (TCNQ) Salts with Metallocene Stacks. *Inorg. Chem.* **1987**, *26* (8), 1328−1331.

https://doi.org/10.1021/jacs.1c07468
J. Am. Chem. Soc. XXXX, XXX, XXX−XXX